PROCEEDINGS OF SCIENCE

Parker Solar Probe Energetic Particle Observations of the September 5, 2022 SEP Event

C.M.S. Cohen[a,*] E.R. Christian[b], A.C. Cummings[a], A.J. Davis[a], G.A. de Nolfo[b], M.I. Desai[c], J. Giacalone[d], M.E. Hill[e], A.W. Labrador[a], R.A. Leske[a], D.J. McComas[f], R.L. McNutt Jr. [e], R.A. Mewaldt[a], D.G. Mitchell[e], J.G. Mitchell[b], J.S. Rankin[f], N.A. Schwadron[e,g], T. Sharma[f], M.M. Shen[f], J.R. Szalay[f], M.E. Wiedenbeck[h], A. Vourlidas[e], S.D. Bale[i], M. Pulupa[i], J.C. Kasper[j], D.E. Larson[i], and P. Whittlesey[i]

[a]*California Institute of Technology, MC 290-17, Pasadena, USA*

[b]*NASA/Goddard Space Flight Center, 8800 Greenbelt Rd, Greenbelt, USA*

[c]*Southwest Research Institute, 6220 Culebra Rd, San Antonio, USA*

[d]*University of Arizona, 1200 E University Blvd, Tucson, USA*

[e]*Johns Hopkins Applied Physics Laboratory, 11100 Johns Hopkins Rd., Laurel, USA*

[f]*Princeton University, PO Box430, Princeton, USA*

[g]*University of New Hampshire, 105 Main St., Durham, USA*

[h]*Jet Propulsion Laboratory, 4800 Oak Grove Dr., La Cañada Flintridge, USA*

[i]*University of California Berkeley, 1 Centennial Dr., Berkeley, USA*

[j]*University of Michigan, 500 S State St., Ann Arbor, USA*

E-mail: cohen@srl.caltech.edu

On 5 September 2022 Parker Solar Probe (Parker) was less than 17 Rs from the Sun when the Integrated Science Investigation of the Sun (ISʘIS) observed an intense solar energetic particle (SEP) event associated with a strong soft x-ray flare and a very fast coronal mass ejection (CME). The energy dependence of the particle onsets indicate shock acceleration both far and close to the spacecraft providing a unique opportunity to study the evolution of particle energization. Significant time variability of the characteristics of the energetic particle population is evident and has been examined in relation to magnetic and plasma structures and expectations from acceleration processes. We present an overview of these observations and highlight a few of the ongoing studies.

38th International Cosmic Ray Conference (ICRC2023)
26 July - 3 August, 2023
Nagoya, Japan

*Speaker

PoS(ICRC2023)1276

1. Introduction

On 5 September 2022, active region 13088 was on the opposite side of the Sun at W180S10 as viewed from Earth. Fortunately, Parker Solar Probe (Parker, [1]) and Solar Orbiter (SolO, [2]) were also beyond the western limb at W118 and W149 respectively. The Extreme Ultraviolet Imager (EUI, [3]) on SolO had an excellent view of the region (Figure 1). At ~15:30 UT the region erupted creating a large x-ray flare, measured in several energy channels by the SolO Spectrometer/Telescope for Imaging X-rays (STIX, [4]) and estimated to be between M9 and X2 on the GOES-class scale. An associated coronal mass ejection (CME) was observed as a halo CME by SOHO/LASCO and STEREO-A/SECCHI. Using STEREO-A/SECCHI/COR-2 data, it was estimated that the CME-driven shock was traveling ~2260 km/s at ~15 R_S (Figure 2).

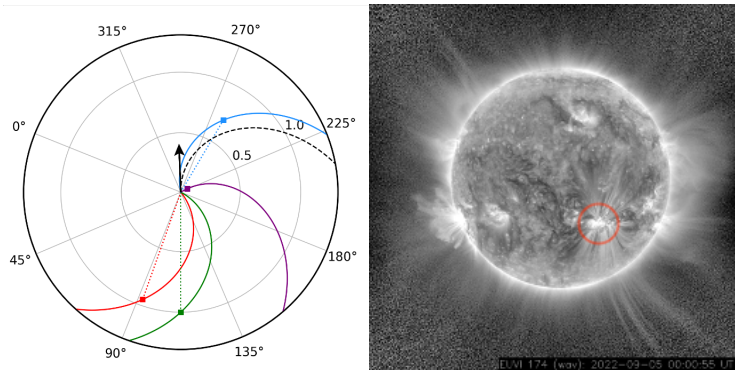

Figure 1. (left) Position of the observing spacecraft at the time of the eruption; STEREO-A (red), ACE (green), Parker (purple), SolO (blue); the arrow indicates the direction of the erupting CME. (right) SolO/EUI observations of the active region (indicated by the red circle).

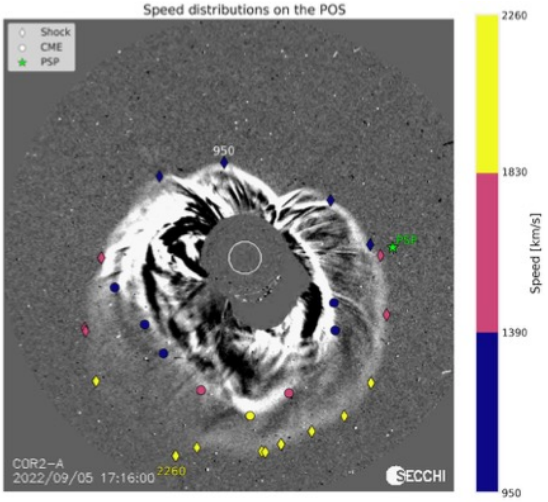

Figure 2. CME as observed by STEREO-A/SECCHI/COR2. Speed estimates are given by the color bar on the right for points along the shock (diamonds) and the CME (circles). The location of Parker is indicated by the green star.

At this time, Parker was at 15 R_S and positioned such that the flank of the CME passed over the spacecraft (Figure 2, see also [5]); the CME was imaged dramatically by the Wide-Field Imager for Solar Probe Plus (WISPR, [6]) coronagraph onboard. SolO at 0.7 AU also encountered

the CME, closer to the nose, and both spacecraft observed large solar energetic particle (SEP) events. Here we present initial observations of this large SEP event at the unprecedented radial distance of Parker.

2. ISOIS Observations

The Integrated Science Investigation of the Sun (ISOIS, [7]) measures energetic particles from ~20 keV to over 100 MeV/nuc with two Energetic Particle Instruments (EPI), EPI-Lo [8] and EPI-Hi [9]. EPI-Lo is a time-of-flight sensor with 80 separate apertures to provide 2π field of view. EPI-Hi consists of two low energy telescopes (LETs) measuring ions from ~1 to 20 MeV/nuc; one double-ended with a sunward facing aperture, LETA, and anti-sunward aperture, LETB, and a single-ended telescope, LETC, pointing orthogonally to LETA. The higher energies (>10 MeV/nuc) are captured by a double-ended high energy telescope (HET) with one side, HETA, pointed sunward and the other, HETB, anti-sunward.

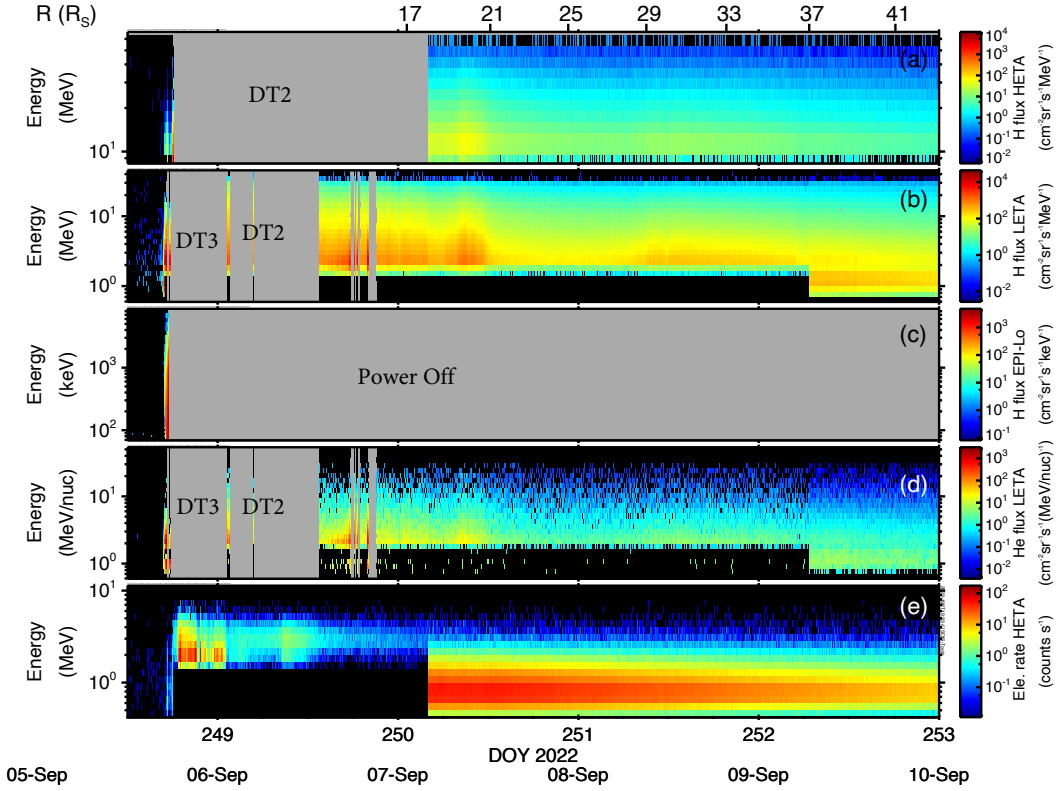

Figure 3. ISOIS energy spectrograms of the event; (a) protons from HETA; (b) protons from LETA; (c) protons from EPI-Lo; (d) helium from LETA; (e) electrons from HETA. Note electrons are presented as counts/sec rather than intensities and EPI-Lo energies are given in keV. Grey regions indicate time periods of dynamic thresholds (HETA and LETA, see text) and EPI-Lo turn off.

Figure 3 provides an overview of the event in energy spectrograms for protons from HETA, LETA, and EPI-Lo (averaged over all apertures), He from LETA and electrons from HETA. Unfortunately, as the particle intensities increased dramatically just before the arrival of the interplanetary shock, EPI-Lo powered off due to an overcurrent detection (significant efforts have been undertaken to prevent this from happening in future large events). The high intensities triggered EPI-Hi to shift to dynamic threshold (DT) modes, as designed. The DT modes involve raising the energy thresholds on various detector segments to limit the energy range of protons,

He, and electrons to which the instrument responds in order to avoid severely decreased instrument livetime. More details on these modes can be found in [9]. To date the instrument calibration for DT2 is not complete and those periods are greyed out in Figure 3.

In DT3, only small 'pixel' segments of some of the detectors remain sensitive to protons (and heavier ions). The pixel rates are accumulated throughout the event (regardless of the instrument DT mode), providing an indication of the ion variability throughout the event. Additional qualitative information can be gained by computing the ratio of the pixel counting rates; e.g., the ratio of the pixel rate of the third detector of LETA to that of the third detector of LETB provides anisotropy information since LETA measures particles traveling away from the Sun and LETB measures particles flowing back towards the Sun. The ratio of the pixel rate of the fourth detector of LETA to that of the third detector of LETA provides information regarding the hardness of the ion spectrum, as the fourth detector responds to ions of a higher energy than the third detector does. Currently, these are only qualitative variations as the pixel rates have not been calibrated to intensities.

The plasma and magnetic field measurements have been analyzed by [5] and several distinct time periods have been identified. Many of the boundaries identified correspond to changes in the SEP characteristics. Here we examine four specific intervals: the SEP event onset, the passage of the interplanetary shock, the sheath region and the passage of the magnetic cloud.

2.1 Event onset

Proton energy spectrograms from HETA, LETA, and EPI-Lo, along with the components and magnitude of the magnetic field from FIELDS [10], are given in Figure 4 for the first few

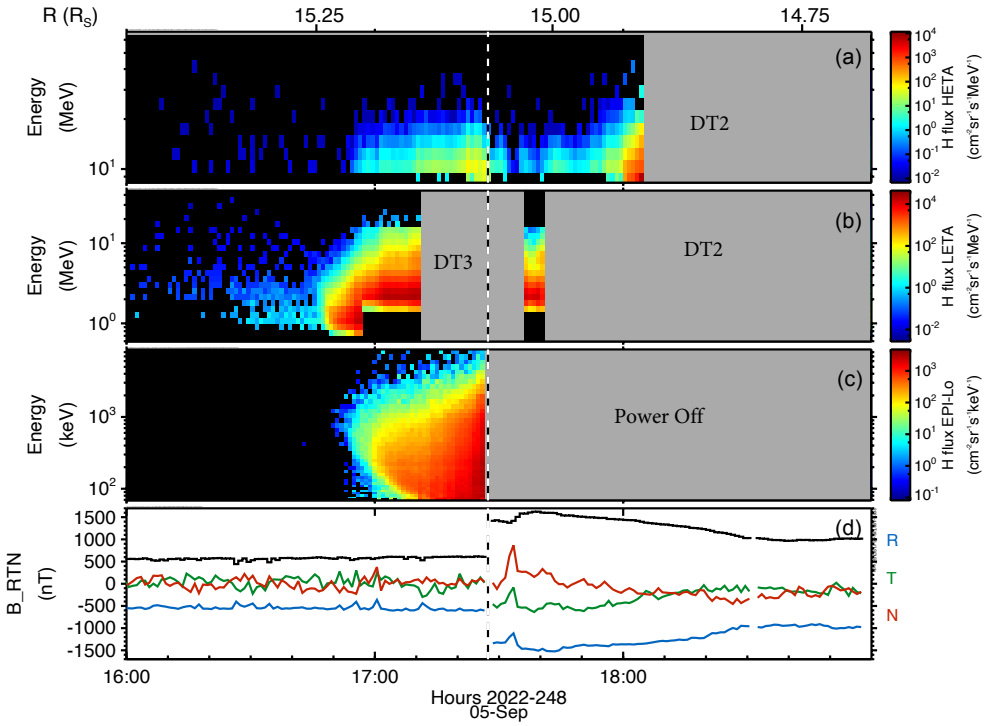

Figure 4. ISOIS energy spectrograms at the onset of the event showing proton data from HETA (a), LETA (b) and EPI-Lo (c). Magnetic field data are given in (d). The vertical line indicates the passage of the interplanetary shock.

hours of the event. The 'nose' feature seen clearly in the EPI-Lo data is a new observation and is being studied in detail by [11]. The lower energy portion (i.e., <1 MeV) corresponds to the velocity dispersion pattern typical of large SEP events where higher energy particles are observed first (due to their higher speed), followed by successively lower energy ones. The higher energy portion of the nose (i.e., >1 MeV) is an aspect that has not been seen in observations near 1 AU; here the higher energy particles are absent at the start of the event, arriving *after* the lower energy particles. This behavior continues in the higher energy ranges measured by LETA and HETA.

The nose can be understood as a result of acceleration times increasing as a function of energy combined with the decreasing distance between the shock and the spacecraft at the time the particles escape the shock. For the 'normal' dispersive part of the nose feature, although the higher energy particles take longer to be accelerated and thus leave the shock later than the lower energy particles, the spacecraft is sufficiently far from the shock that the higher energy particles can overtake the lower ones and reach the spacecraft first. For the upper part of the nose, the acceleration time is sufficiently long for the higher energy particles that once they escape the shock, they do not have enough time to overtake the lower energy particles before reaching the spacecraft and thus are detected later.

Figure 5 presents more data from HET and LET. The left panel shows several engineering rates from HET; these are combined for HETA and HETB and as a function of depth in the instrument (i.e., R1 is the rate measured by the first detectors and R4 is the rate measured by the fourth detectors; the approximate energy ranges are given in the legend). In the right panel, several ratios of pixel rates are shown which indicate changes in spectral hardness (panel a) and flow direction (from LET in panel b and from HET in panel c). An increase in the ratios shown in panel a indicates a hardening of the spectra and, correspondingly, a decrease implies softening. A horizontal line at a value of 1 is drawn in panels b and c; above this line, more particles are traveling away from the Sun, below this line more are flowing towards the Sun. As is evident from Figures 4 and 5, few particles >20 MeV (as observed by HET) are present upstream of the shock. At lower energies, the LETA/LETB ratios indicate that the SEPs are predominantly traveling away from the Sun as expected. This anisotropy increases as the shock approaches, while the spectra appear to soften.

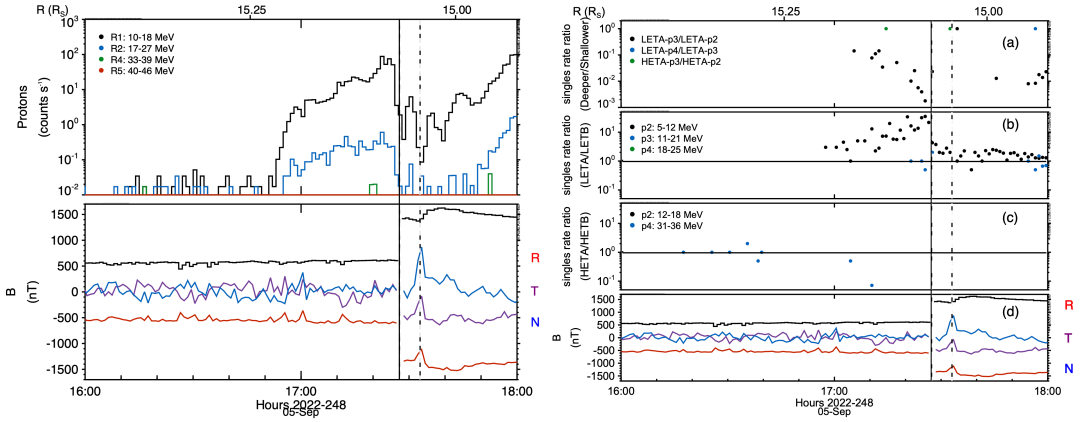

Figure 5. (left) Proton engineering rates for HET detectors (approximate energy ranges are indicated)(top); magnetic field data (bottom). (right) ratio of pixel rates from LETA and HETA (a); ratios of LETB/LETA pixel rates (b); ratios of HETB/HETA pixel rates (c); magnetic field data (d). The shock arrival time is given by the solid vertical lines and the end of the sheath by dashed vertical lines as determined by [5].

2.2 Shock passage and sheath region

The arrival of the shock is evident by the sharp increase in the magnetic field magnitude (black trace in bottom panels of Figure 5), occurring at 17:27 on 5 September, as marked by the vertical solid lines. It can be seen in the upper panel of the left plot of Figure 5 that the high energy proton counting rates drop dramatically just before the arrival of the shock. Clearly the shock either is not strong enough or has not had enough time to accelerate significant numbers of high energy particles as it passes over Parker. From the right plot it is clear that the particle distribution becomes significantly more isotropic at the time of the shock passage (panel b) and continues to soften (panel a). In an analysis of the heavy ion spectra [12], the power-law spectral index at this time is close to -9, which is extremely soft.

The identified sheath region is quite short, starting with the shock passage and ending just 6 minutes later at 17:33 (dashed vertical lines). The shortness of the sheath region might be because at 15 R_S, significant separation due to the speed differential between the CME and the shock has yet to develop. During this time period the SEP counting rates peak temporarily, followed by a dip that appears to be strongly inversely correlated with the short-lived increase in all the magnetic field components which marks the end of the sheath. This local change in the magnetic field may be acting as a barrier, trapping the SEPs between it and the shock upstream, explaining the increase in particle counting rates and shift to a more nearly isotropic distribution.

2.3 Magnetic cloud

Figure 6 shows the period of time when the magnetic cloud passes over Parker on 5 and 6 September. Just inside the leading edge of the cloud, HET shifts to DT2 and the lower energy traces (from the first and second detectors, labeled R1 and R2) in the top panel of the left plot drop to zero due to the detector thresholds being raised. However, the steady increase in the proton rates just before the DT transition can be seen; coincident with this increase is the appearance of the higher energy protons, which continue to increase dramatically in counting rate as Parker moves farther into the cloud and remains high to the end of the cloud passage. As is apparent from the right plot, significant hardening of the spectra accompanies this increase and the particle distributions are most often isotropic. However, there are several distinct periods early in the cloud passage where, particularly for the lower energies (panel b), the dominant flow

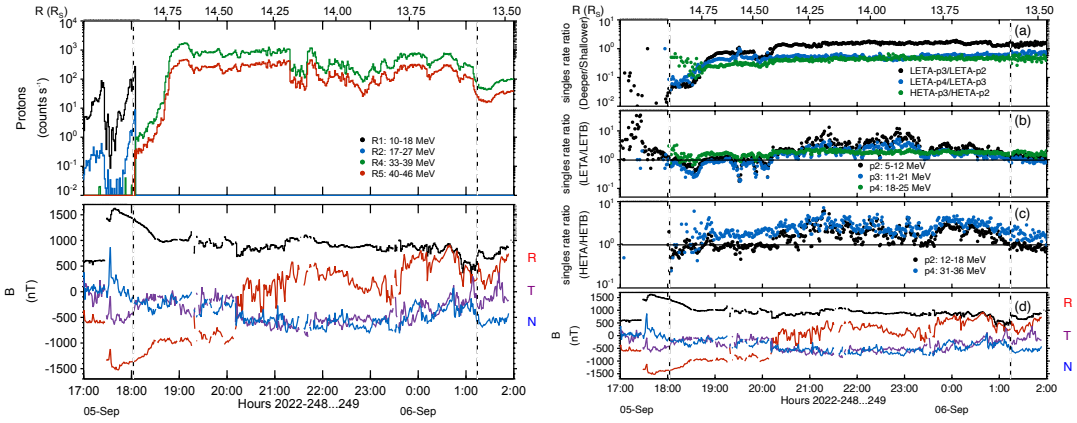

Figure 6. Same format as for Figure 5 but for the magnetic cloud period (beginning and end of the magnetic cloud are indicated by the dashed lines.

direction is back towards the Sun (by factors of several). At higher energies (panel c) the distribution is either isotropic or primarily flowing away from the Sun. There are no obvious changes in the magnetic field components that correspond to these periods of unusual flow direction at the lower energies.

3.Discussion

The 5 September 2022 SEP event was the first large, shock-accelerated event observed inside 15 R_S. The ISʘIS suite measured protons up to at least 60 MeV. Although EPI-Lo turned off shortly before the arrival of the shock, the onset of the event was captured in substantial detail, revealing an energy dependence to the first arriving particles that has never been seen at 1 AU. A comprehensive analysis of the onset, including modeling efforts to understand and simulate the key features, is presented in [11].

The ion characteristics, including intensities, spectra, composition, and anisotropies, vary substantially through the event. Interestingly, many of the changes are well correlated with plasma features identified separately by [5]; a more complete analysis of this is currently ongoing. Particularly unexpected is the strong drop in SEP intensities just before the shock arrival, the confinement of the >30 MeV protons to the magnetic cloud, and the periods of strong sunward flow inside the magnetic cloud. Such features are not typical in SEP events observed at 1 AU and may provide insights regarding particle acceleration and transport very near the Sun.

It is curious that the sheath region is substantially shorter than that characteristically seen at 1 AU, lasting only 6 minutes (note: [5] identified the arrival of the magnetic cloud approximately 30 minutes after the end of the sheath, but even if one considers this period as part of the sheath, 36 minutes is still unusually short, see e.g., [13]). It is possible this is merely a consequence of the shock having not yet propagated away from the magnetic cloud ejecta by a significant amount. Within this narrow region, there is an isotropic population of SEPs that may be trapped between the shock and the magnetic field increase marking the end of the sheath region. This has some similarities to an unusual event observed by Parker at 0.76 AU on 30 June 2021 [14], which also had a strong particle enhancement in the sheath region suggestive of particle energization via processes internal to the sheath. However, in that event, the particle enhancement was limited to lower energies, < 0.5 MeV, and the sheath region was quite turbulent and lasted for 7.2 hours. Increased turbulence in the short sheath region of this event is not clear, suggesting that trapping may be a better explanation for the particle enhancement than local acceleration.

Finally, it should be noted that this event was observed by other spacecraft. In particular SolO measured a strong SEP event as well as the associated interplanetary shock and CME. Preliminary work shows that the shock at SolO was significantly different in orientation and strength from that at Parker [15]. This is perhaps not surprising given that SolO crossed the CME closer to the nose, while Parker intercepted the flank. Comparisons of the SEP characteristics (particularly associated with the shock passage) are currently underway. Initial analysis of the heavy ion composition suggests that the event was also substantially different at the two spacecraft, with Parker observing overall an Fe-poor (relative to O) population and SolO measuring an Fe-rich one (albeit at lower energies than the Parker observations). Much work remains to relate these compositional differences to various conditions sampled by the two spacecraft, including evolving magnetic connections to the shock and the state of the background solar wind into which the shock propagated.

Acknowledgments

This work was supported by NASA contract NNN06AA01C, and benefited greatly from the many individuals who have contributed to make Parker such a successful mission. Parker Solar Probe was designed, built, and is now operated by the Johns Hopkins Applied Physics Laboratory as part of NASA's Living with a Star (LWS) program.

References

[1] N.J. Fox, et al. *The Solar Probe Plus Mission: Humanity's First Visit to Our Star*, *SSRv*, **204** (2016) 7.

[2] D. Müller, et al. *The Solar Orbiter mission. Science overview, A&A,* **642** (2020) [doi: 10.1051/0004-6361/202038467].

[3] P. Rochus et al., *The Solar Orbiter EUI instrument: The Extreme Ultraviolet Imager, A&A*, **642** (2020) [10.1051/0004-6361/201936663].

[4] S. Krucker, et al., *The Spectrometer/Telescope for Imaging X-rays (STIX), A&A*, **642** (2020) [10.1051/0004-6361/201937362].

[5] O.M. Romeo, et al., *Near-Sun In situ and Remote Sensing Observations of a CME and its Effect on the Heliospheric Current Sheet, ApJ,* in press (2023).

[6] A. Vourlidas et al., *The Wide-Field Imager for Solar Probe Plus (WISPR), SSRv*, **204** (2016) 83, [10.1007/s11214-014-0114-y].

[7] D.J. McComas et al., *Integrated Science Investigation of the Sun (ISIS): Design of the Energetic Particle Investigation, SSRv*, **204** (2016) 187 [10.1007/s11214-014-0059-1].

[8] M.E. Hill et al., *The Mushroom: A half-sky energetic ion and electron detector, JGR*, **122** (2017) 1513 [10.1002/2016ja022614].

[9] M.E. Wiedenbeck et al., *Capabilities and Performance of the High-Energy Energetic-Particles Instrument for the Parker Solar Probe Mission, Proc. 35th Internat. Cosmic Ray Conf. (ICRC2017)* **301** (2017) 16.

[10] S. Bale, et al. *The FIELDS Instrument Suite for Solar Probe Plus. Measuring the Coronal Plasma and Magnetic Field, Plasma Waves and Turbulence, and Radio Signatures of Solar Transients, SSRv*, **204** (2016) 49 [10.1007/s11214-016-0244-5].

[11] M.E. Hill, et al., in preparation (2023).

[12] R.A. Leske, et al., *ApJ,* in preparation (2023).

[13] E. Kilpua et al. *Statistical Analysis of Magnetic Field Fluctuations in Coronal Mass Ejection-Driven Sheath Regions, Front. Astron. Space Sci.,* **7** (2021) [10.3389/fspas.2020.610278].

[14] E. Kilpua, et al., *Energetic ion enhancements in sheaths driven by interplanetary coronal mass ejections, Astron. & Sp. Sci.*, in press (2023) [10.1007/s10509-023-04201-6].

[15] D. Trotta, private communication, June 2023.